Soret and Dufour Effects on Magneto-Nanofluid Flow Over a Stretching Sheet in the Presence of Thermal Radiation and Heat Generation/Absorption

T. RangaRao[1], S Sathies Kumar[2], K. Gangadhar[3],
[1]Department of Mathematics, SVKP College, Markapur, Prakasam DT-523316, India
[2] Department of Mathematics, Raghava Degree College, Ongole, A. P.-523001, India
[3] Department of Mathematics, Acharya Nagarjuna University, Ongole, A. P.-523001, India

Abstract.
This study investigates the results of soret and dufour on boundary layer magneto-nanofluid flow over a extending sheet in the company of thermal radiation and heat source/sink. The leading partial differential equations are changed to a system of ordinary differential equations and worked out numerically using fourth order Runge-Kutta method together with shooting technique. The results of the magnetic influence number, the Prandtl number, Lewis number, the Brownian motion parameter, thermophoresis parameter, radiation parameter, heat source/sink parameter, the soret number and the Dufour number on the fluid properties in addition to on the heat, regular and nano mass transfer coefficients are concluded and exposed graphically.

Keywords: *nanofluid, Radiation, MHD, heat source/sink, Brownian motion, thermophoresis.*

1.Introduction

Natural convection heat transfer in enclosures is an key observable fact in engineering systems owing to its large functions in building heating, automotive technology, solar technology cooling of electronic equipment, etc [1-3]. Development in the heat transfer presentation of these structures is an necessary theme as of an energy reduction viewpoint. Together with this aspire, an inventive method to improve heat transfer tempo by means of nanoscale particles (smaller than 100 nm) balanced in the base fluid, has appeared. Engineered suspensions of nanoparticles in liquids, recognized freshly as nanofluid, have produced significant attention for their possible to develop the heat transfer rate in engineering systems. Nanofluids are ready from a variety of substances, for example oxide ceramics (Al2O3, CuO), nitride ceramics (AlN, SiN), carbide ceramics (SiC, TiC), metals (Cu, Ag, Au), semiconductors, (TiO2, SiC), carbon nanotubes, and compound materials for instance alloyed nanoparticles or nanoparticle core–polymer shell composites [4]. The support medium of nanofluids is regularly water, oil, acetone, decene, ethyleneglycol, etc. Compared with conventional heat transfer for instance oil, water and ethylene glycol mixture, nanofluids have appreciably superior thermal conductivity that accordingly develops the heat move characteristics of these fluids. Aminreza Noghrehabadi and Amin Samimi [5] considered the natural convection heat transfer of nanofluids owing to thermophoresis and brownian diffusion in a square enclosed space.

In accordance with the majority of the prior studies, the MHD flow has established the concentration of lots of investigators because of its business purposes. In metallurgy, for pattern, a few procedures engage the cooling of several uninterrupted bands by sketch them from end to end an electrically conducting fluid expose to a magnetic field (Kandasamy and Muhaimin [6]).This permits the tempo of cooling to be restricted and last product through the wanted features to be gained. A further significant appliance of hydromagnetic flow in metallurgy is in the refinement of molten metals as of nonmetallic additions during the purpose of a magnetic field. Research has also been carried out by previous researchers on the flow and heat transfer consequences of electrically conducting fluids such as liquid metals, water mixed with a little acid and other corresponding substance before a magnetic field. The studies have involved different geometries and different boundary conditions. Herdricha et al. [7] studied MHD flow control for plasma technology applications. They identified prospective uses for magnetically managed plasmas in the fields of space technology plus in plasma technology. Seddeek et al. [8] investigated the similarity solution in MHD flow and heat transfer over a wedge in view of uneven viscosity and thermal conductivities. Aydin and Kaya [9] studied MHD mixed convection of a viscous dissipating fluid about a permeable vertical flat plate and found that the value of Richardson number determines

the effect of the magnetic parameter on the momentum and heat transfer. Abd El-Gaied and Hamad [10] investigated the MHD forced convection laminar boundary layer flow of alumina-water Nanofluid in excess of a stirring permeable flat plate with convective face boundary condition. The magnetohydrodynamic (MHD) forced convection boundary layer flow of nanofluid over a horizontal stretching plate was examined by Nourazar et al. [11] by means of homotopy perturbation method (HPM).

Thermal radiation of a gray fluid which is releasing and attracting radiation in a non-scattering middling was argued by Hossain et al [12]. Partial slip effects on boundary layer flow past a permeable exponential stretching sheet in presence of thermal radiation was examined by Mukhopadhyay et al. [13]. Alam et al. [14] explored the property of variable suction and thermophoresis on steady MHD combined free-forced convective heat and mass transfer flow over a semi-infinite permeable inclined plate in front of thermal radiation. Sandeep et al. [15] considered the effects of radiation on an unsteady natural convective flow of an EG-Nimonic 80a nanofluid past an infinite vertical plate.

Natural convection in square hollow space with two pairs of heat source–sink packed with water–CuO nanofluid statistically executed by Aminossadati and Ghasemi [16]. They terminated that the rate of heat transfer amplifies with raise of the Rayleigh number and the solid volume fraction in both cases of the location of the couple of source–sink. Yu et al. [17] looked into transient natural convection heat transfer of aqueous nanofluids in a discrepancy heated square cavity. They finished that the time–middling Nusselt number is inferior with growing volume fraction of nanoparticles at invariable Rayleigh numbers. Hamad and Pop [18] offered in their fresh paper that the solid volume and heat source improves the heat transfer rate. Hady et al. [19] calculated the natural convection boundary-layer flow over a downward-pointing vertical cone in a porous medium saturated with a non-Newtonian nanofluid in front of heat generation or absorption. The numerical modelling of the conjugate heat transfer and fluid flow of Al2O3/water nanofluid during the microchannel heat sink was offered by Lelea [20]. Shahi et al. [21] studied the effect of Rayleigh number, solid concentration and heat source location on entropy generation because of natural convection of a nanofluid in a cavity with a projected heat source. Rahman and Salahuddin [22] considered the outcomes of uneven electric conductivity and viscosity on hydromagnetic heat and mass transfer flow by the side of a radiated isothermal inclined permeable surface in a stationary fluid which contains internal heat generation. Das [23] calculated the influence of partial slip, thermal radiation and temperature dependent fluid properties on the hydro-magnetic fluid flow and heat transfer over a flat plate with heat generation. Srikanth et al. [24] explored the MHD convective heat transfer of a nano fluid flow past an inclined permeable plate with heat source and radiation.

Additionally, the thermal-diffusion (Soret) effect, for example, has been developed for isotope division, and in combinations among gases with extremely less molecular weight (Hz, He) and of average molecular weight (Nz, air) the diffusion-thermo (Dufour) effect was found to be of a substantial amount such that it cannot be unnoticed, explained by Eckert and Drake [25] in their book. Mahabub et al. [26] investigated the Soret-Dufour results on the MHD flow and heat transfer of Microrotation fluid over a Nonlinear stretching plate in the company of suction. Recently, Awad et al. [27] studied the Thermo diffusion effects on magneto-nanofluid flow above a stretching sheet.

However, the interaction of Soret and Dufour consequences in a magneto-nanofluid flow over a stretching sheet, has established small concentration. Hence, the current reading is an effort to scrutinize the steady thermodiffusion outcomes in a magneto- nanofluid flow above a stretching sheet in the company of thermal radiation and heat source/sink. The prevailing boundary layer equations have been changed to a two-point boundary value problem in similarity variables and the resulting problem is answered numerically with the fourth order Runge-Kutta method together with shooting technique. The consequences of variety of governing constraints on the fluid velocity, temperature, concentration, nanoparticle volume friction, reduced Nusselt number, Sherwood number and nanofluid Sherwood number are exposed in figures and examined in depth .

2. Mathematical Formulation

Think about two-dimensional nanofluid flow over a linearly stretching sheet with velocity $u_w = ax$, where a is a real positive number. The coordinate system is assumed to describe the x-axis by the side of the exterior of the sheet and y is the coordinate perpendicular to the surface of the sheet. A consistent magnetic field of potency B0 is affected normal to the plate parallel to y-direction and that the stimulated magnetic field is ignored, which is acceptable for MHD flow at little magnetic Reynolds number. The surface temperature T_w and nanoparticle concentration $\hat{\phi}_w$ are superior than the ambient values T_∞ and $\hat{\phi}_\infty$, correspondingly. Under these suppositions together with the Boussinesq and boundary layer approximations, the system of equations, governing the flow field are specified by

Continuity equation

$$\frac{\partial u}{\partial x}+\frac{\partial v}{\partial y}=0 \tag{2.1}$$

Momentum equation

$$u\frac{\partial u}{\partial x}+v\frac{\partial u}{\partial y}=\upsilon\frac{\partial^2 u}{\partial y^2}-\frac{\sigma B_0^2}{\rho_f}u \tag{2.2}$$

Energy equation

$$u\frac{\partial T}{\partial x}+v\frac{\partial T}{\partial y}=\alpha\frac{\partial^2 T}{\partial y^2}-\frac{1}{\rho_f c_p}\frac{\partial q_r}{\partial y}$$

$$+\tau\left[D_B\frac{\partial\hat{\phi}}{\partial\hat{y}}\frac{\partial T}{\partial\hat{y}}+\frac{D_T}{T_\infty}\left(\frac{\partial T}{\partial y}\right)^2\right]+D_{TC}\frac{\partial^2 C}{\partial y^2}+\frac{q_0}{\rho_f c_p}(T-T_\infty) \tag{2.3}$$

Species equation

$$u\frac{\partial C}{\partial x}+v\frac{\partial C}{\partial y}=D_S\frac{\partial^2 C}{\partial y^2}+D_{CT}\frac{\partial^2 T}{\partial y^2} \tag{2.4}$$

Nanofluid Volume friction equation

$$u\frac{\partial\hat{\phi}}{\partial x}+v\frac{\partial\hat{\phi}}{\partial y}=D_B\frac{\partial^2\hat{\phi}}{\partial y^2}+\left(\frac{D_T}{T_\infty}\right)\frac{\partial^2 T}{\partial y^2} \tag{2.5}$$

The boundary conditions for the velocity, temperature and concentration fields are

$$u=u_w=ax, v=0, T=T_w, C=C_w, \hat{\phi}=\hat{\phi}_w \quad \text{at} \quad y=0$$

$$u\to 0, T\to T_\infty, C\to C_\infty, \hat{\phi}\to\hat{\phi}_\infty \quad \text{as} \quad \hat{y}\to\infty \tag{2.6}$$

where u and v are the velocity factors along the x and y axes, correspondingly, T is the fluid temperature and C is the solutal concentration, $\hat{\phi}$ is the nanopartical volume fraction, $(\rho c)_f$ and $(\rho c)_p$ are the heat capacity of the fluid and the effective heat capacity of the nanoparticle material respectively, υ is the kinematic viscosity of the base fluid, B_0 is the magnetic field of constant strength, q_r is the radiative heat flux, α is the thermal diffusivity of the porous medium, D_B is the Brownian diffusion coefficient, D_{CT} and D_{TC} are theSoret and Dufour diffusivities, σ is the electrical conductivity, D_S is the solutal diffusivity, τ is a parameter defined by $(\rho c)_f/(\rho c)_p$, q_0 is the heat source/sink constant.

By using the Rosseland approximation (Brewster [28]), the radiative heat flux qr is specified by

$$q_r=-\frac{4\sigma_1}{3k_1}\frac{\partial T^4}{\partial y} \tag{2.7}$$

where σ_1 is the Stefan-Boltzmann constant and k_1 - the mean absorption coefficient. It should be distinguished that by using the Rosseland estimate, the current study is restricted to optically thick fluids. If temperature diversities inside the flow are suitably minute, then the equation (2.7) can be linearized by expanding T^4 into the Taylor series about T_∞, which after ignoring higher order terms takes the form

$$T^4\cong 4T_\infty^3T-3T_\infty^4 \tag{2.8}$$

Considering the equations (2.7) and (2.8), the equation (2.4) changes to

$$u\frac{\partial T}{\partial x}+v\frac{\partial T}{\partial y}=\alpha\left(1+\frac{16\sigma_1T_\infty^3}{3k_1k}\right)\frac{\partial^2 T}{\partial y^2}+\tau\left[D_B\frac{\partial\hat{\phi}}{\partial\hat{y}}\frac{\partial T}{\partial\hat{y}}+\frac{D_T}{T_\infty}\left(\frac{\partial T}{\partial y}\right)^2\right]+D_{TC}\frac{\partial^2 C}{\partial y^2}+\frac{q_0}{\rho_f c_p}(T-T_\infty) \tag{2.9}$$

The continuity equation (2.1) is fulfilled by the Cauchy Riemann equations

$$u = \frac{\partial \psi}{\partial y} \quad \text{and} \quad v = -\frac{\partial \psi}{\partial x} \tag{2.10}$$

where $\psi(x, y)$ is the stream function.

So as to transform the equations (2.2), (2.4), (2.5) and (2.9) into a set of ordinary differential equations, the following similarity transformations and dimensionless variables are established.

$$\psi = (a\upsilon)^{1/2} f(\eta), \eta = y\sqrt{\frac{a}{\upsilon}}, \theta(\eta) = \frac{T - T_\infty}{T_w - T_\infty}, S(\eta) = \frac{C - C_\infty}{C_w - C_\infty}$$

$$\phi(\eta) = \frac{\hat{\phi} - \hat{\phi}_\infty}{\hat{\phi}_w - \hat{\phi}_\infty}, M = \frac{\sigma B_0^2}{\rho_f a}, \Pr = \frac{\upsilon}{\alpha}, Le = \frac{\upsilon}{D_S}, Rd = \frac{16\sigma_1 T_\infty^3}{3k_1 k}$$

$$Nb = \frac{\tau D_B(\hat{\phi}_w - \hat{\phi}_\infty)}{\upsilon}, Nt = \frac{\tau D_T(T_w - T_\infty)}{T_\infty \upsilon}, Ln = \frac{\upsilon}{D_B}$$

$$Nd = \frac{D_{TC}(C_w - C_\infty)}{\alpha(T_w - T_\infty)}, Ld = \frac{D_{CT}(T_w - T_\infty)}{D_S(C_w - C_\infty)}, Q = \frac{q_0}{a\rho_f c_p} \tag{2.11}$$

where $f(\eta)$ is the dimensionless stream function, θ - the dimensionless temperature, S - the dimensionless concentration, ϕ - the dimensionless nanoparticle volume fraction, η - the similarity variable, M - the magnetic parameter, Le - the Lewis number, Nb - the Brownian motion parameter, Nt - the thermophoresis parameter, Ln - the nanofluid Lewis number, Nd - modified Dufour number, Pr - the Prandtl number, Ld - the Dufour solutal Lewis number, Q- heat source/sink parameter and Rd- the radiation parameter.

In consideration of the equations (2.10) and (2.11), the equations (2.2), (2.4), (2.5) and (2.9) change into

$$f''' + ff'' - f'^2 - Mf' = 0 \tag{2.12}$$

$$(1 + Rd)\theta'' + \Pr f\theta' + \Pr Nb\theta'\phi' + \Pr Nt\theta'^2 + \Pr Q\theta + NdS'' = 0 \tag{2.13}$$

$$S'' + LefS' + Ld\theta'' = 0 \tag{2.14}$$

$$\phi'' + Lnf\phi' + \frac{Nt}{Nb}\theta'' = 0 \tag{2.15}$$

The transformed boundary conditions can be written as

$$f = 0, f' = 1, \theta = 1, S = 1, \phi = 1 \quad \text{at} \quad \eta = 0$$

$$f' \to 0, \theta \to 0, S \to 0, \phi \to 0 \quad \text{as} \quad \eta \to \infty \tag{2.16}$$

The parameters of engineering attention in heat and mass carrying problems are the local Nusselt number Nux, the Sherwood number Shx and the nanofluid Sherwood number Shx,n. These parameters describe the wall heat, the regular and nano mass transfer rates, correspondingly, and are defined by

$$Nu_x = \frac{-x}{T_w - T_\infty}\left(\frac{\partial T}{\partial y}\right)\Big|_{y=0} = -\mathrm{Re}_x^{1/2}\theta'(0)$$

$$Sh_x = \frac{-x}{C_w - C_\infty}\left(\frac{\partial C}{\partial y}\right)\Big|_{y=0} = -\mathrm{Re}_x^{1/2} S'(0)$$

$$Sh_{x,n} = \frac{-x}{\hat{\phi}_w - \hat{\phi}_\infty}\left(\frac{\partial \hat{\phi}}{\partial y}\right)\Big|_{y=0} = -\mathrm{Re}_x^{1/2}\phi'(0) \tag{2.17}$$

Following Khan and Aziz [29], the physical parameters of concern are the reduced Nusselt Nur, the Sherwood number Sh and the reduced Sherwood Shr defined as

$$Nur = Nu_x / \mathrm{Re}_x^{1/2}, Sh = Sh_x / \mathrm{Re}_x^{1/2} \quad \text{and} \quad Shr = Sh_{x,n} / \mathrm{Re}_x^{1/2} \tag{2.18}$$

3. Solution Of The Problem

The set of non-linear coupled differential Eqs. (2.12)-(2.15) subject to the boundary conditions Eq. (2.16) represent a two-point boundary value problem. So as to work out these equations numerically we follow the majority specialized numerical shooting technique with fifth-order Runge-Kutta-integration scheme. In this method it is mostly necessary to choose the appropriate restricted values of $\eta \to \infty$. To choose η_∞ we begin with a little early approximation value and reply the problem with different particular set of parameters to get f'', θ', S' and ϕ'. The solution process is recurring with an extra large value of η_∞ up to two successive values of f'', θ', S' and ϕ' differ just after desired digit signifying the limit of the boundary along η. The previous value of η_∞ is selected as appropriate value of the limit $\eta \to \infty$ for that meticulous set of parameters. The four ordinary differential Eqs. (2.12)-(2.15) were first originated as a set of seven first-order instantaneous equations of seven unknowns following the method of superposition [30]. Thus, we set

$$y_1 = f, y_2 = f', y_3 = f'', y_4 = \theta, y_5 = \theta', y_6 = S, y_7 = S', y_8 = \phi, y_9 = \phi'$$

$$y_1' = y_2, y_2' = y_3$$

$$y_1(0) = 0, y_2(0) = 1$$

$$y_3' = y_2^2 + M y_2 - y_1 y_3$$

$$y_3(0) = \delta_1$$

$$y_4' = y_5, y_4(0) = 1$$

$$y_5' = \left(\frac{-\Pr}{(1 + Rd)} \right) \left[y_1 y_5 + N b y_5 y_9 + N t y_5^2 + Q y_4 + N d y_7' \right]$$

$$y_5(0) = \delta_2$$

$$y_6' = y_7, y_6(0) = 1$$

$$y_7' = -\left[Le y_1 y_7 + L d y_5' \right]$$

$$y_7(0) = \delta_3$$

$$y_8' = y_9, y_8(0) = 1$$

$$y_9' = -\left[L n y_1 y_9 + \frac{N t}{N b} y_5' \right]$$

$$y_9(0) = \delta_4$$

Eqs. (2.12)-(2.15) then reduced into a system of ordinary differential equations, i.e., where $\delta_1, \delta_2, \delta_3$ and δ_4 are determined such that it satisfies $y_2(\infty) \to 0, y_4(\infty) \to 0, y_6(\infty) \to 0$ and $y_8(\infty) \to 0$. The shooting method is familiar with presumption $\delta_1, \delta_2, \delta_3$ and δ_4 until the boundary conditions $y_2(\infty) \to 0, y_4(\infty) \to 0, y_6(\infty) \to 0$ and $y_8(\infty) \to 0$ are satisfied. Then the resulting differential equations can be integrated by fifth-order Runge-Kutta integration scheme. The above process is recurring until we obtain the results up to the preferred degree of correctness, 10^{-6}

4. Results and Discussion

So as to get a understandable insight of the physical problem, the velocity, temperature and concentration have been argued by giving numerical values to the governing parameters come upon in the problem. Numerical computations are shown from figures.1-18.

The velocity components f and f' are designed in Figures. 1 and 2 for diverse values of the magnetic field parameter (M). As is now well known, the velocity reduces with raises in the magnetic field parameter because of an raise in the Lorentz drag force that resists the fluid motion.

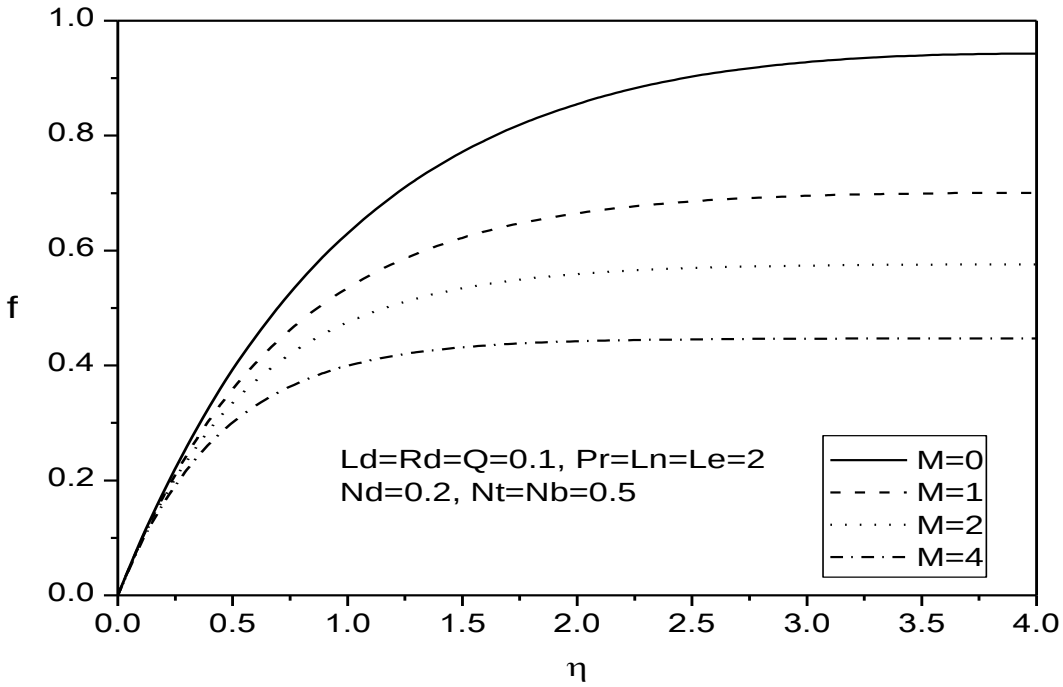

Figure.1 Velocity component f for diverse values of M

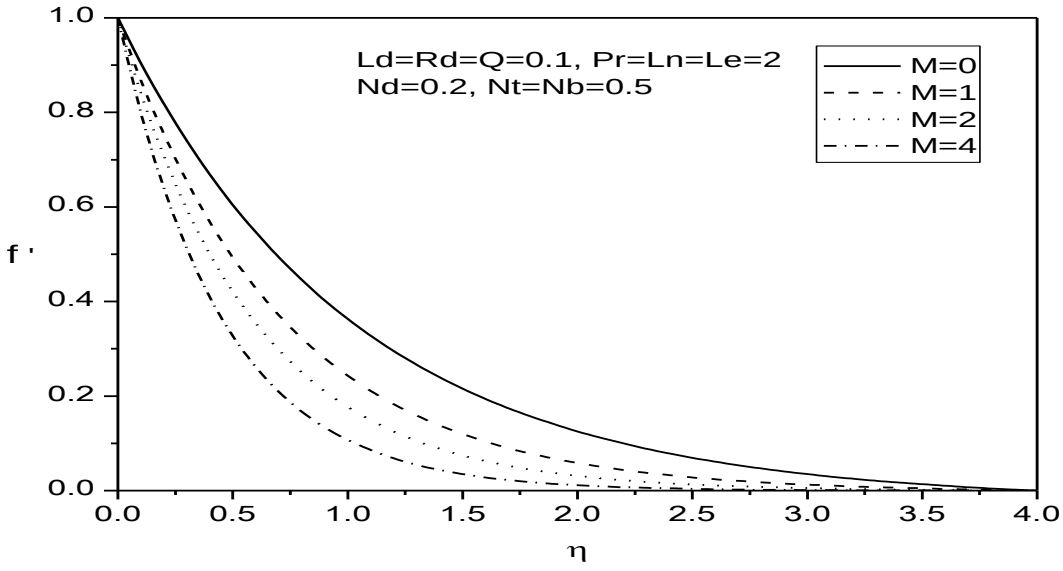

Figure.2 Velocity component f' for diverse values of M

Figures.3 and 4 explain the consequence of the thermophoresis parameter on the temperature as well as mass volume fraction profiles. The thermophoretic force produced by the temperature gradient produces a quick flow away from the stretching surface. In this fashion more fluid is heated clear of the surface, and as a result, as Nt enhances, the temperature inside the boundary layer raises. The quick flow from the stretching sheet takes with it nanoparticles show the way to an raise in the mass volume fraction boundary layer thickness.

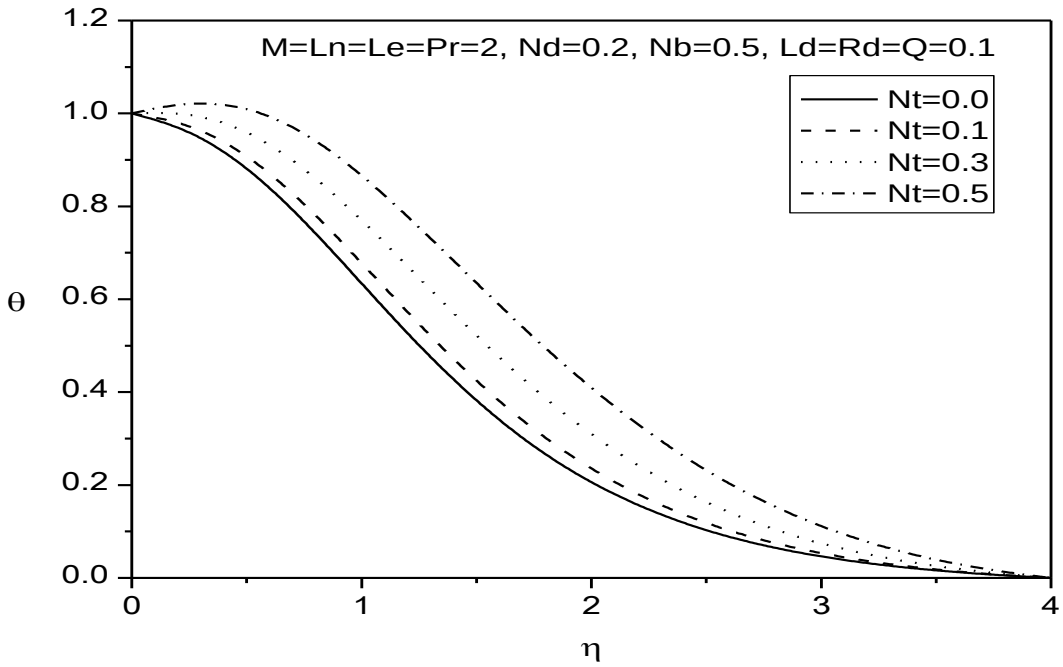

Figure.3 Temperature θ profiles for various values of Nt

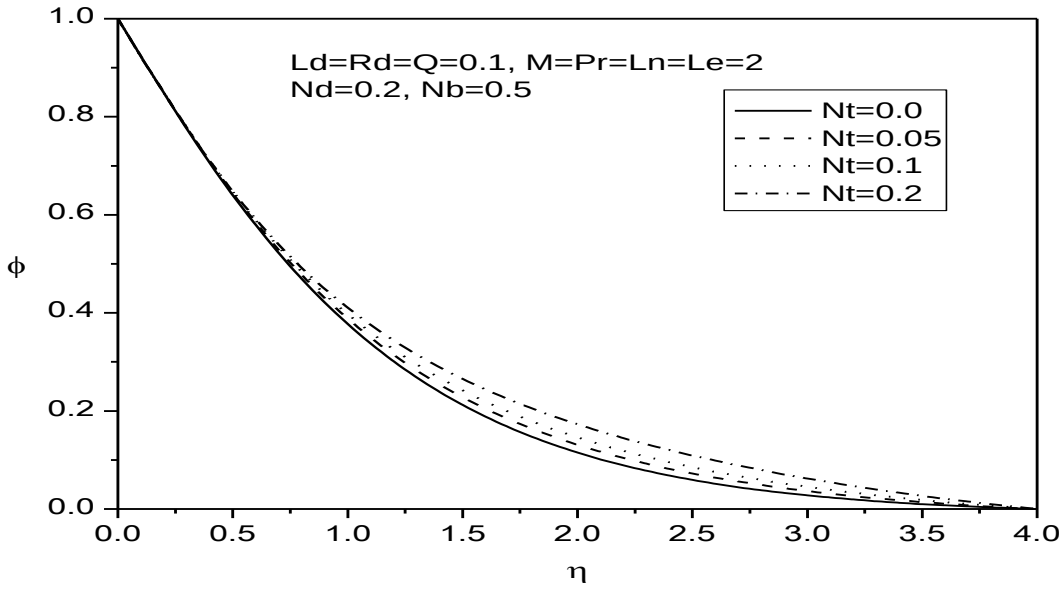

Figure.4 Nanoparticle ϕ profiles for different values of Nt

The result of the Brownian motion of the nanoparticles hanging in the fluid on the temperature and nanoparticle volume fraction is revealed in Figures. 5 and 6. As predicted the improved Brownian motion of the nanoparticles takes with it heat and the thickness of the thermal boundary layer increases. The Brownian motion of the nanoparticles increases thermal transport which is an important mechanism for the improvement of thermal conductivity of nanofluids. Though, we note that rising the Brownian motion parameter directs to a gathering of the nanoparticles close to the stretching sheet. An raise in the Brownian motion of the nanoparticles guides to a reduce in the mass volume fraction profiles.

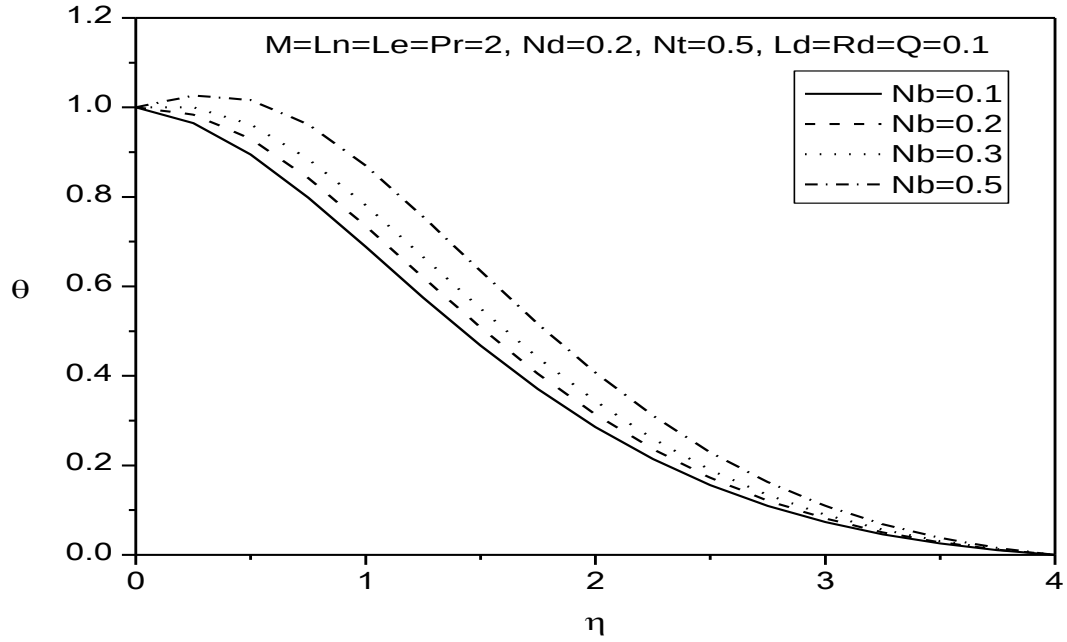

Figure.5 Temperature θ profiles for various values of Nb

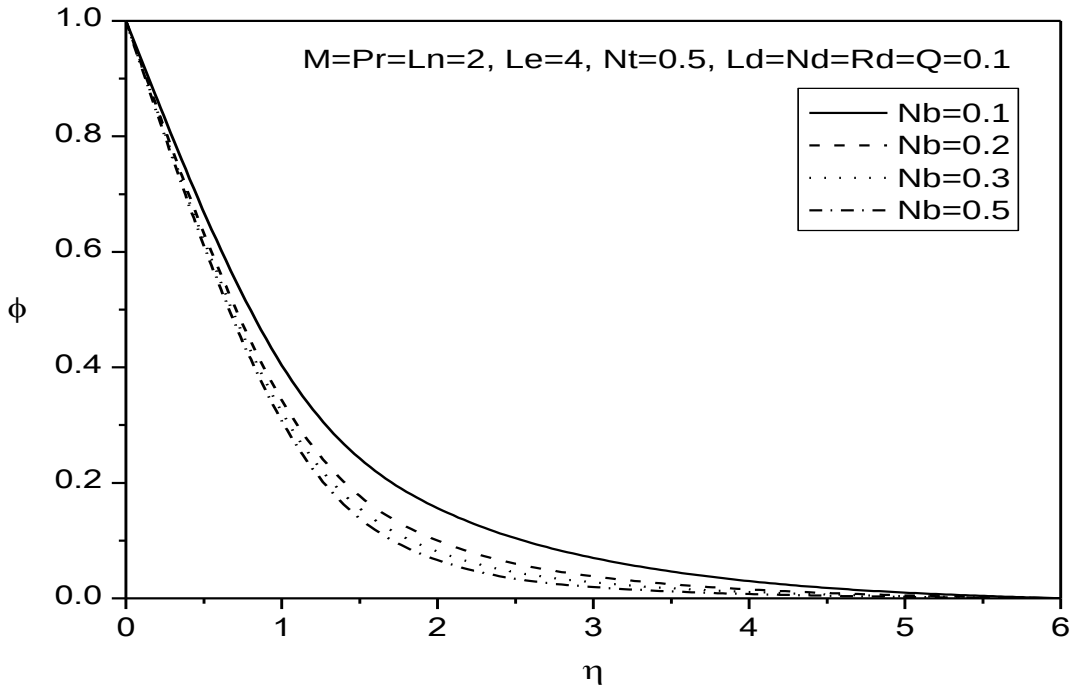

Figure.6 nanoparticle ϕ profiles for various values of Nb

Figures. 7 and 8 illustrate the effect of the Lewis number (Le), and the Dufour-solutal Lewis number (Ld) on the species concentration in the boundary layer. The concentration profiles appreciably contract as the Lewis number raises and the Dufour-solutal Lewis number reduces.

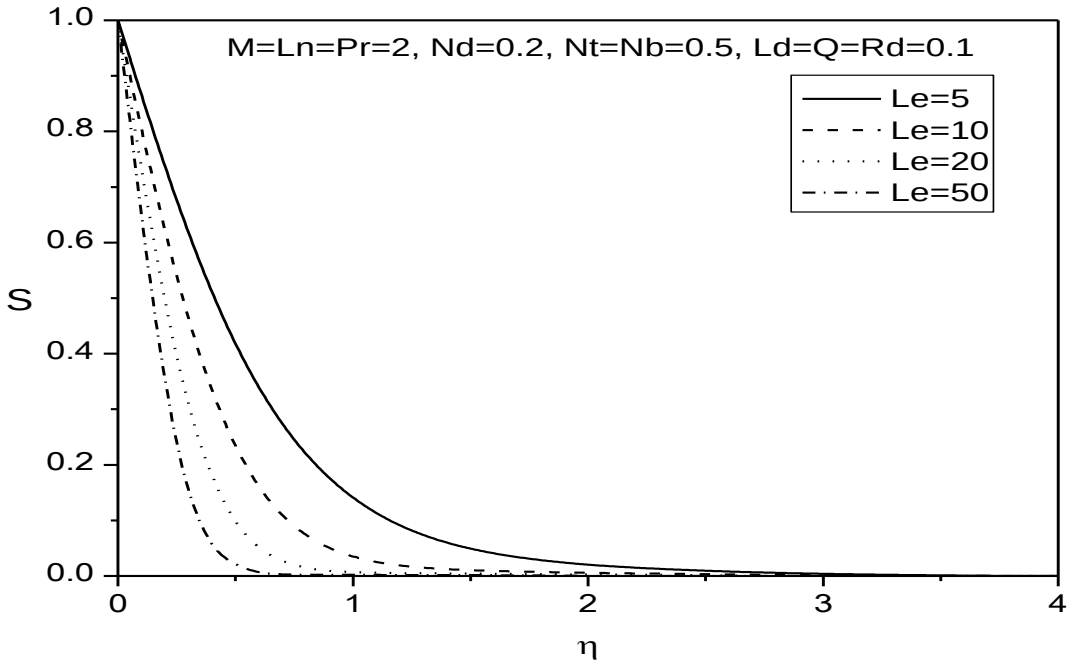

Figure.7 Concentration S profiles for diverse values of Le

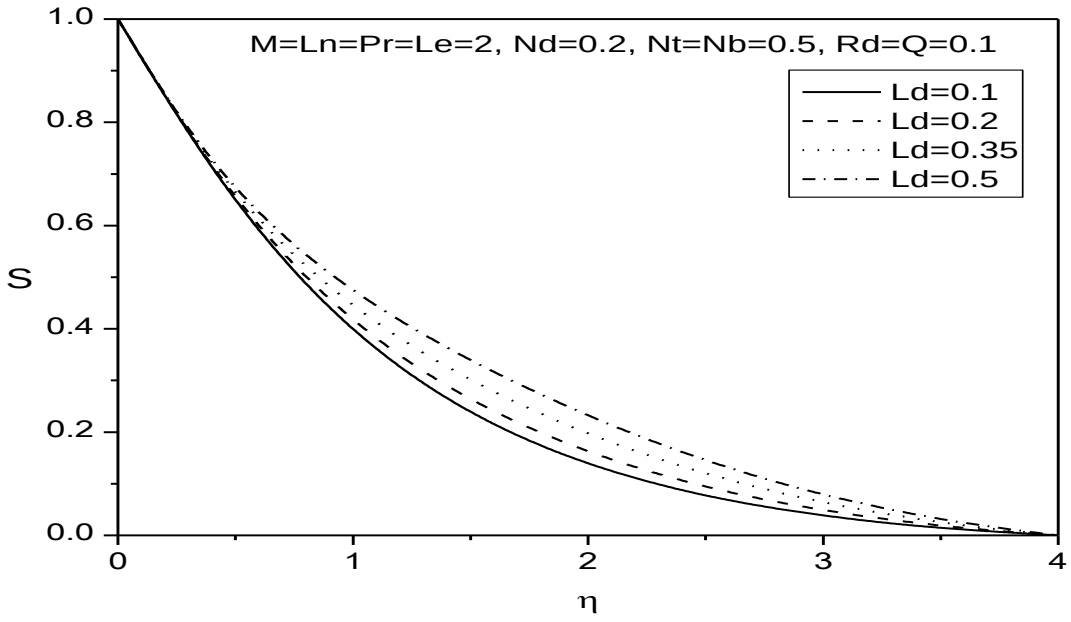

Figure.8 Concentration S profiles for diverse values of Ld

Figures. 9 and 10 explain the temperature profiles for several values of the Prandtl number Pr and modified Dufour number Nd. The temperature profiles decline as the Prandtl number boosts since, for elevated Prandtl numbers, the flow is managed by momentum and viscous diffusion rather than thermal diffusion. Conversely, the thickness of the thermal boundary layer raises with an raise in Nd.

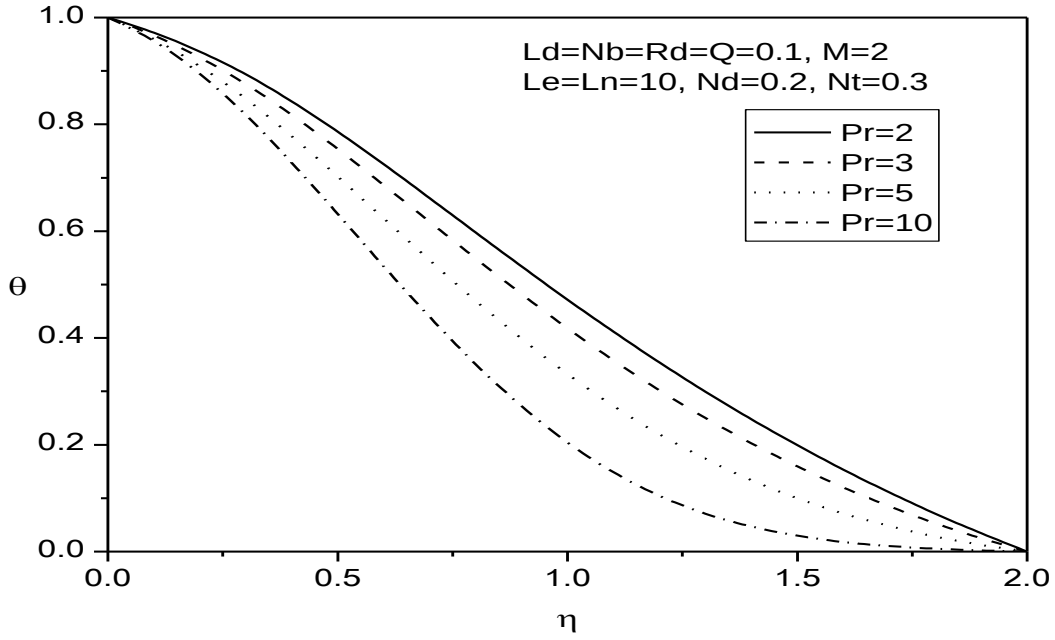

Figure.9 Temperature θ profiles for diverse values of Pr

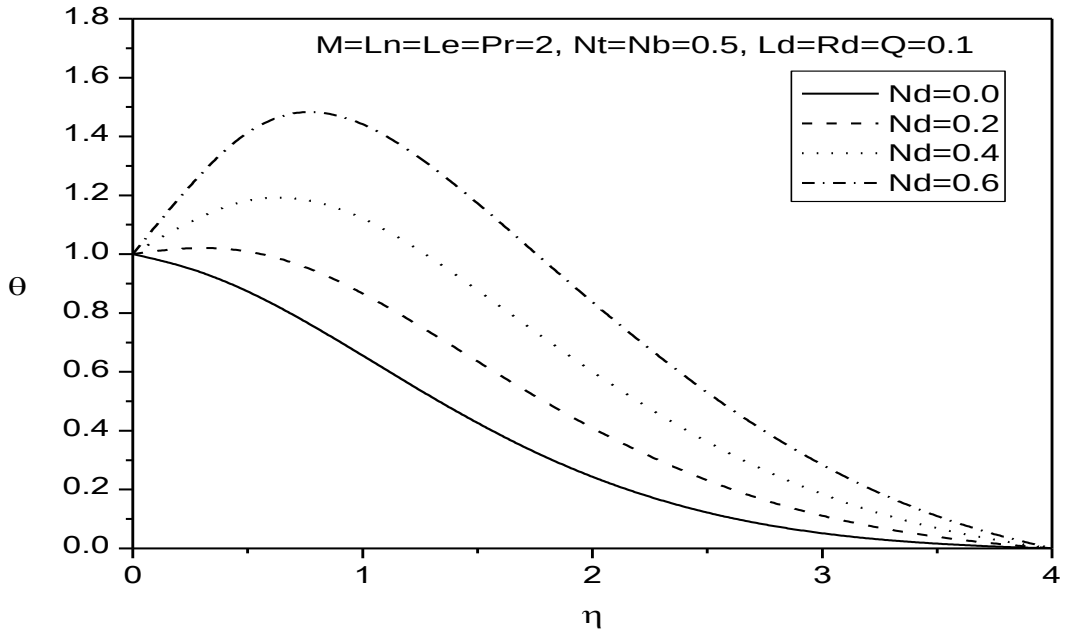

Figure.10 Temperature θ profiles for diverse values of Nd

Figures. 11 and 12 confirm the effect of the radiation parameter (Rd), and the heat source/sink parameter (Q) on the temperature profiles. The temperature profiles notably enhance as the radiation parameter and heat source/sink parameter enhances.

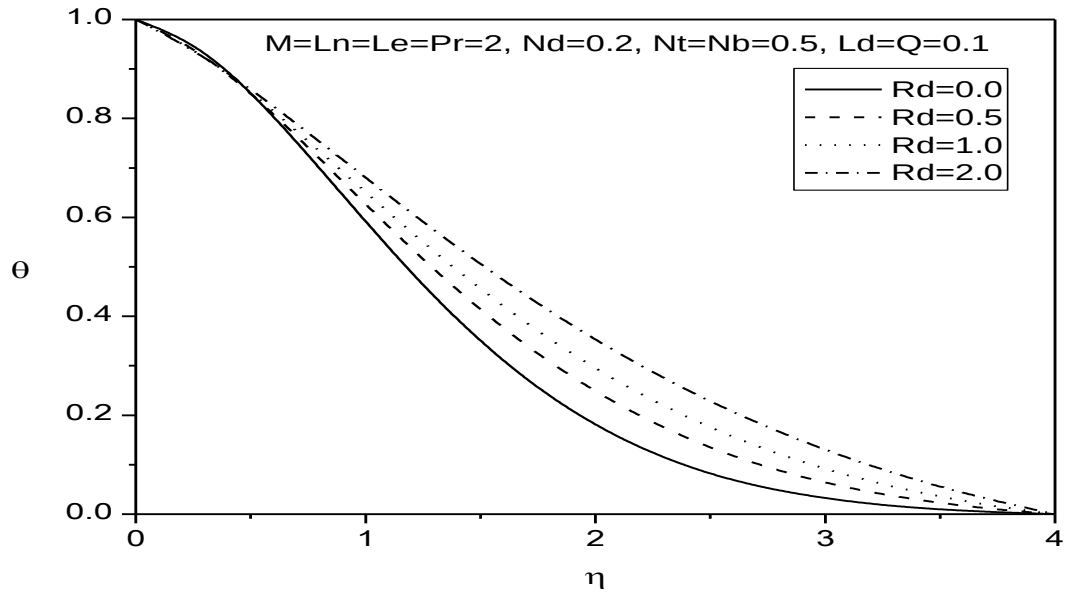

Figure.11 Temperature θ profiles for diverse values of Rd

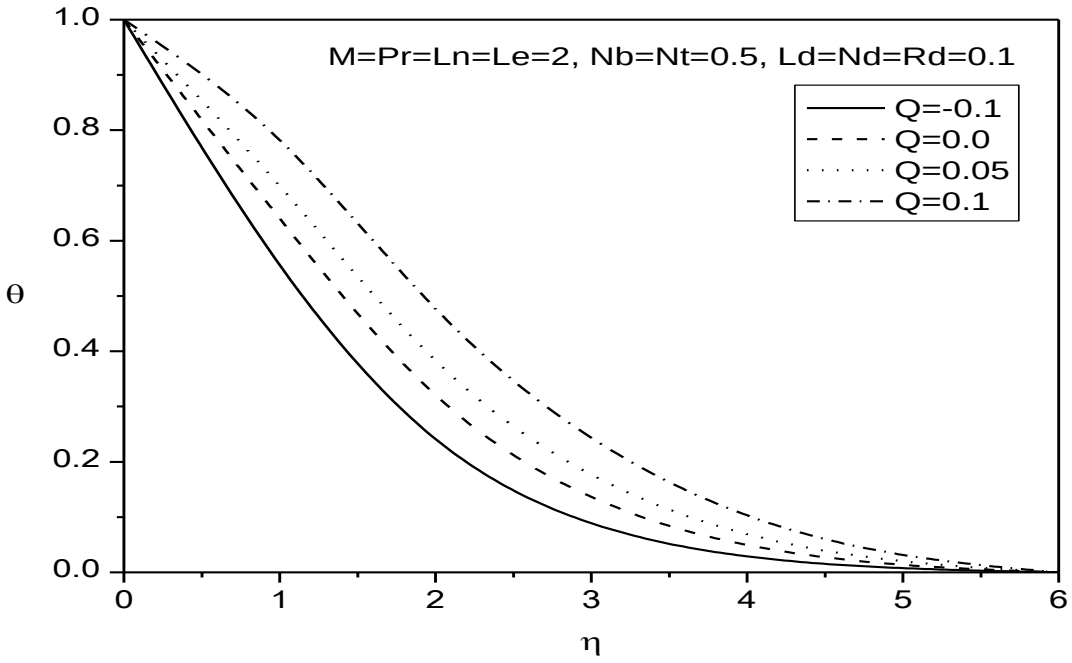

Figure.12 Temperature θ profiles for diverse values of Q

Figures. 13 confirm the effects of the thermophoresis parameter Nt, the heat source/sink parameter Q on the wall heat fraction transfer rate. It can be seen that the thermal boundary layer thickness boosts when the thermophoresis parameter Nt enlarges, thus lessening the reduced Nusselt number. Though rising the heat source/sink parameter guides to a reduce in the reduced Nusselt number.

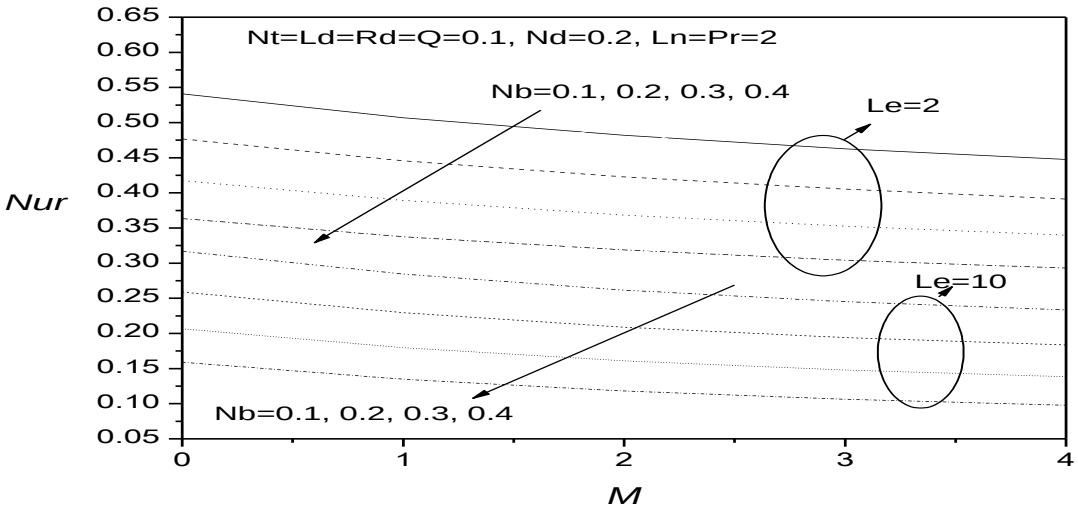

Figure.13 Effect of Nb, Le and M on the condensed Nusselt number Nur

Figures. 14 demonstrate the effects of the Brownian motion parameter, Lewis number and the magnetic parameter on the decreased Nusselt number Nur. We note down a reduce in the reduced Nusselt number when Nb or Le or M raises.

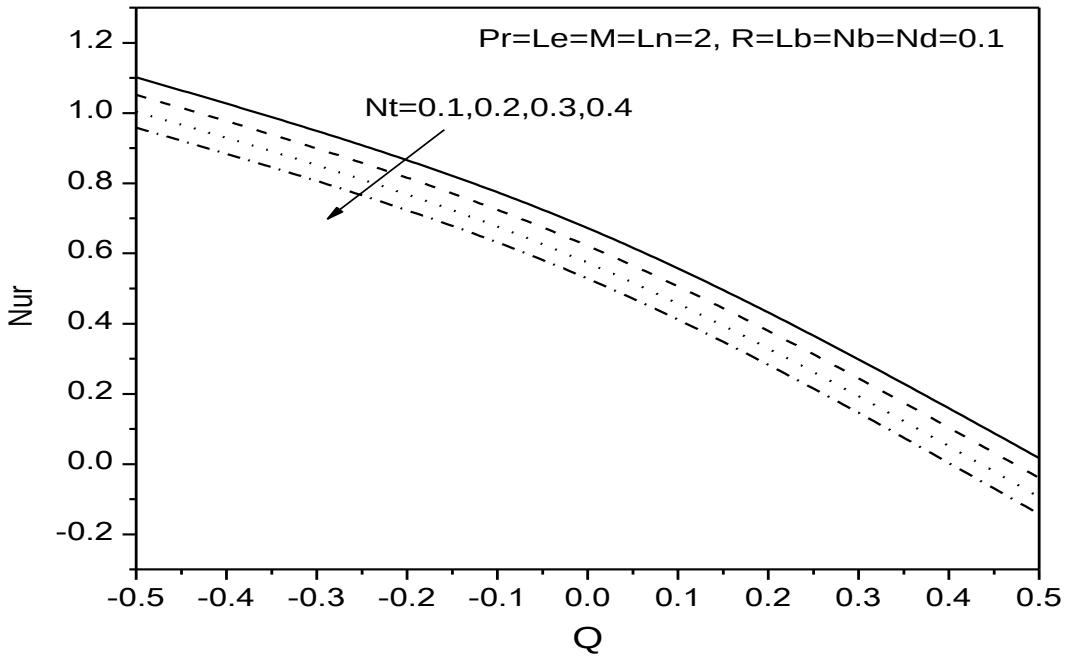

Figure.14 Effect of Nt and Q on the decreased Nusselt number Nur

Figures. 15 and 16 illustrate the effects of the thermophoresis parameter, Brownian motion parameter and Lewis number on the local Sherwood number $-S'(0)$. We examine an raise in the $-S'(0)$ when Nt or Nb or Le raises.

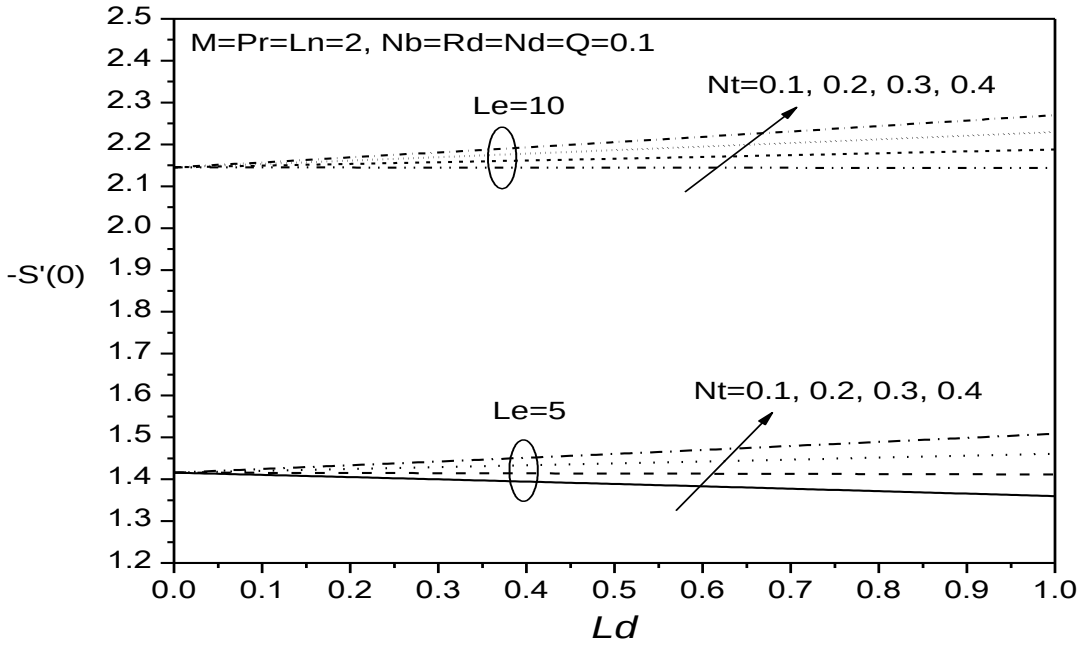

Figure.15 Effect of Nt, Le and Ld on the local Sherwood number $-S'(0)$

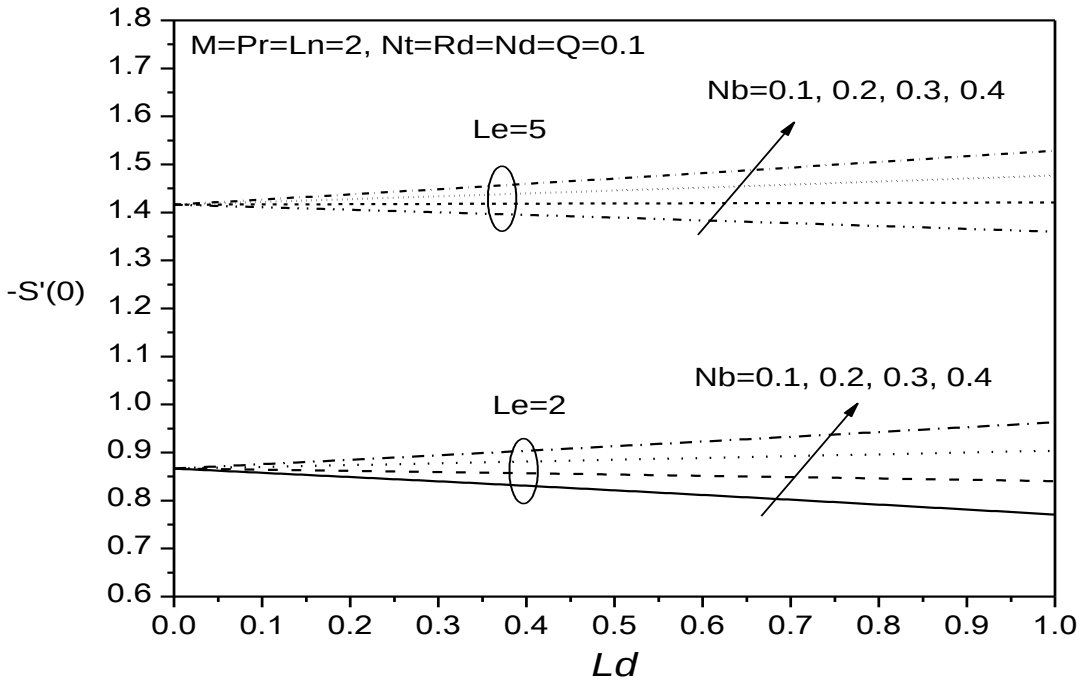

Figure.16 Effect of Nb, Le and Ld on the local Sherwood number $-S'(0)$

Figures. 17 and 18 dipicts the effects of the thermophoresis parameter, Brownian motion parameter and nanofluid Lewis number on the nanofluid Sherwood number $-\phi'(0)$. We observe an increase in the $-\phi'(0)$ when Nt or Nb or Ln increases.

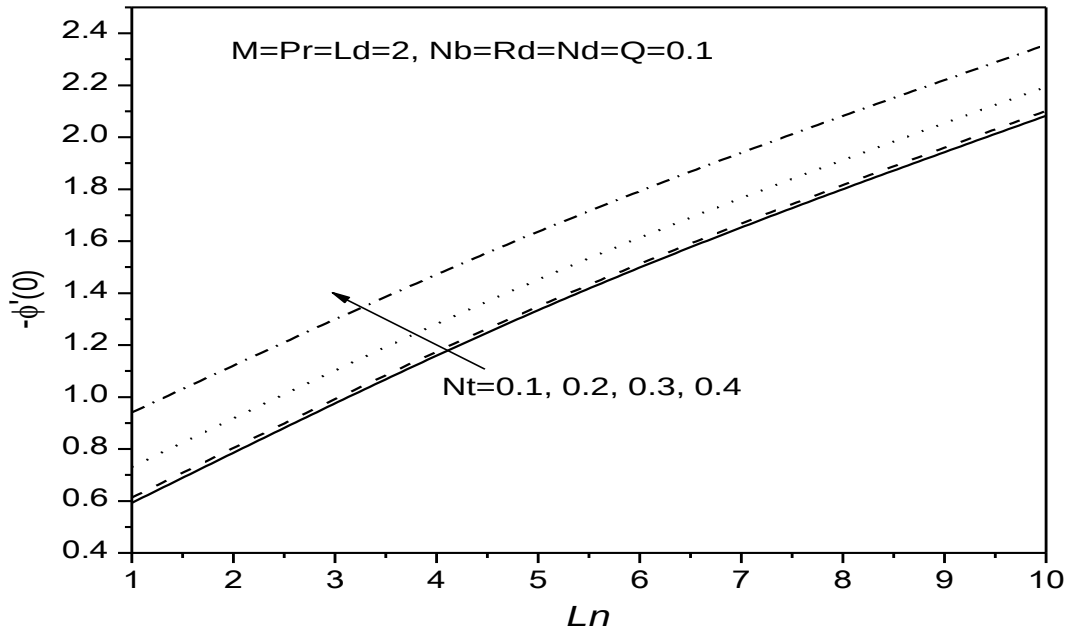

Figure.17 Effect of Nt and Ln on the nanofluid Sherwood number $-\phi'(0)$

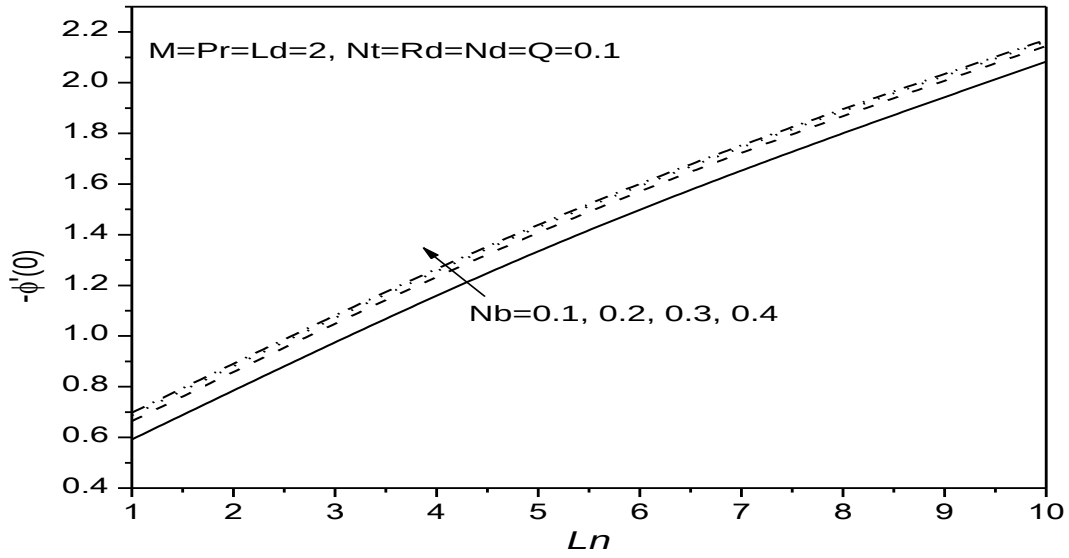

Figure.18 Effect of Nb and Ln on the nanofluid Sherwood number $-\phi'(0)$

5. Conclusion

In the present numerical study, the radiating and magneto-nanofluid boundary layer flow over a stretching sheet in the company of heat generation or absorption. We concluded the results of different parameters on the fluid properties in addition to the heat, and the usual and nano mass transfer rates. We have exposed that growing the magnetic field parameter M tends to slow down the fluid flow inside the boundary layer. The consequences of

the Prandtl number, the Lewis number, the Brownian motion parameter, the thermophoresis parameter, the nanofluid Lewis number, radiation parameter, heat source/sink parameter, the modified Dufour parameter and the Dufour-solutal Lewis number on the heat, regular and nano mass transfer coefficients and fluid flow characteristics have been calculated. We have examined that:

- The thermal boundary layer thickness raises by means of the thermophoresis parameter.
- Rising the Lewis number and heat source/sink parameter decreases the heat transfer coefficient.
- Rising the radiation and heat source/sink parameters improves the thermal boundary layer thickness

References

[1] VahlDavis and G.D 1962 Natural Convection Of Air in a Square Cavity, A Benchmark Numerical Solution, *Internat. J. Numr. Methods Fluids* Vol. **3** pp. 249–264

[2] Fusegi, T., Hyun, J. M., Kuwahara, K. and Farouk B 1991 A Numerical Study of Three Dimensional Natural Convection in a Differentially Heated Cubical Enclosure, *Int. J. Heat MassTransfer* Vol. **34** pp. 1543–1557

[3] Barakos, G., Mitsoulis and E. 1994 Natural Convection Flow in a Square Cavity revisited: Laminar and Turbulent Models With Wall Functions *Internat. J. Numer. Methods Fluids* Vol. **18** pp. 695–719

[4] Jashim Uddin, Md., Khan, W. A., Ismail and A. I. Md. 2012 Review Article Scaling Group Transformation for MHD Boundary Layer Slip Flow of a Nanofluid over a Convectively Heated Stretching Sheet with Heat Generation, *Mathematical Problems in Engineering*, Vol. **2012**, doi:10.1155/2012/934964

[5] Aminreza Noghrehabadi and Amin Samimi 2012 Natural Convection Heat Transfer of Nanofluids Due to Thermophoresis and Brownian Diffusion in a Square Enclosure, *International Journal of Engineering and Advanced Technology (IJEAT)*, Vol.**1**, Issue-6

[6] Kandasamy, R., Muhaimin and I.2010 Scaling Transformation For the Effect of Temperature-Dependent Fluid Viscosity With Thermophoresis Particle Deposition On MHD-Free Convective Heat and Mass Transfer Over a Porous Stretching Surface, *Transport in Porous Media*, Vol. **84** No. 2 pp. 549–568

[7] Herdricha, G., Auweter-Kurtza, M., Fertiga, M., Nawaza, A., Petkowa and D.2006 MHD Flow Control For Plasma Technology Applications, *Vacuum* Vol. **80** pp. 1167–1173

[8] Seddeek, M. A., Afify, A. A., aHanaya and M. A. 2009 Similarity Solutions For Steady MHD Falkner-Skan Flow and Heat Transfer Over a Wedge by Considering the Effect of Variable Viscosity and Thermal Conductivity, *Applications and Applied Mathematics*, Vol. **4** pp. 301–313

[9] Aydin, O.,a Kaya andA 2009 MHD Mixed Convection of a Viscous Dissipating Fluid About a Permeable Vertical Flat Plate, *Applied Mathematical Modelling*, Vol. **33** No. 11 pp. 4086–4096

[10] Abd El-Gaied, S. M., Hamad and M. A. A. 2013 MHD Forced Convection Laminar Boundary Layer Flow of Alumina-Water Nanofluid over a Moving Permeable Flat Plate with Convective Surface Boundary Condition, Hindawi Publishing Corporation, *Journal of Applied Mathematics*, Vol.**2013**, pp.1-8

[11] Nourazar, S.S., Matin, M.H., Simiari and M. 2011 The HPM Applied to MHD Nanofluid Flow over a Horizontal Stretching Plate, *J. Appl. Math*., **2011**: doi:10.1155/2011/876437

[12] Hossain, M. A., Khanafer, K. Vafai and K. 2001 The effect of radiation on free convection flow of fluid with variable viscosity from a porous vertical plate, *Int. J. Therm. Sci*., Vol.**40**, pp.115–124

[13] Mukhopadhyay, S., Gorla andR.S.R 2012 Effects of Partial Slip On Boundary Layer Flow Past a Permeable Exponential Stretching Sheet in Presence of Thermal Radiation, *Heat Mass Transfer*, Vol.**48** pp.1773–1781

[14] Alam, M.S., Rahman, M.M., Sattar and M. A. 2008 Effects of Variable Suction and Thermophoresis on Steady MHD Combined Free Forced Convective Heat and Mass Transfer Flow over a Semi-Infinite Permeable Inclined Plate in the Presence of Thermal Radiation, *International Journal of Thermal Sciences*, Vol. **47** No. 6 pp. 758–765

[15] Sandeep, N., Sugunamma, V., and Mohan Krishna, P. 2013 Effects of Radiation on an Unsteady Natural Convective Flow of a EG-Nimonic 80a Nanofluid Past an Infinite Vertical Plate, *Advances in Physics Theories and Applications*, Vol.**23** pp.36-43

[16] Aminossadati, S.M., Ghasemi and B. 2011 Natural Convection of Water – CuO Nanofluid in a Cavity with Two Pairs of Heat Source –Sink, *International Communications in Heat and Mass Transfer*, Vol. **38** pp.672 –678

[17] Yu, Z.T., Wang, W., Xu, X., Fan, L.W., Hu, Y.C., Cen and K.F. 2011 A Numerical Investigation of Transient Natural Convection Heat Transfer of Aqueous Nanofluids in a Differentially Heated Square Cavity, *International Communications in Heat and Mass transfer*, Vol. **38** No. 5 pp. 585–589

[18] Hamad, M.A.A., Pop and I. 2011 Unsteady MHD Free Convection Flow Past a Vertical Permeable Flat Plate in a Rotating Frame of Reference with Constant Heat Source in a Nano-fluid, *Heat Mass Transfer, Vol.***47** pp.1517– 1524

[19] Hady, F. M., Ibrahim, F. S., Abdel-Gaied, S. M., Eid and M. R. 2011 Effect of Heat Generation/Absorption on Natural Convective Boundary-Layer Flow Froma Vertical Cone Embedded in a Porous Medium Filled with a Non-Newtonian Nanofluid, *International Communications in Heat and Mass Transfer*, Vol. **38** No. 10 pp. 1414–1420

[20] Lelea and D. 2011 The performance Evaluation of Al2O3/Water Nanofluid Flow and Heat Transfer in Microchannel Heat Sink, *International Journal of Heat and Mass Transfer*, Vol. **54** No. 17-18 pp. 3891–3899

[21] Shahi, M., Mahmoudi, A.H., Raouf and A.H. 2011 Entropy Generation due to Natural Convection Cooling of a Nanofluid, *International Communications in Heat and Mass Transfer*, Vol. **38** No. 7 pp. 972–983

[22] Rahman, M. M., Salahuddin and K.M. 2010 Study of Hydromagnetic Heat and Mass Transfer Flow Over an Inclined Heated Surface with Variable Viscosity and Electric Conductivity, *Communications in Nonlinear Science and Numerical Simulation*, Vol. **15** No. 8, pp. 2073–2085

[23] Das, K. 2012 Impact of Thermal Radiation on MHD Slip Flow Over a Flat Plate with Variable Fluid Properties, *Heat and Mass Transfer*, Vol. **48** pp.767–778

[24] Srikanth, G.V.P.N., Srinivas, G., Reddy and B.R.K. 2013 MHD Convective Heat Transfer of a Nano Fluid Flow Past an Inclined Permeable Plate with Heat Source and Radiation, *International Journal of Physics and Mathematical Sciences*, Vol. **3 (1)** pp.89-95

[25] Eckert, E. R. G., Drake and R. M. 1972 "Analysis of Heat and Mass Transfer," *McGraw-Hill*, New York

[26] Md Abdullah Al Mahbub, Nasrin Jahan Nasu, Shomi Aktar and Zillur Rahman, 2013 Soret-Dufour Effects on the MHD Flow and Heat Transfer of Microrotation Fluid over a Nonlinear Stretching Plate in the Presence of Suction, *Applied Mathematics*, Vol. **4** pp.864-875

[27] Faiz G Awad, Precious Sibanda and Ahmed A Khidir 2013 Thermodiffusion Effects on Magneto-Nanofluid Flow over a Stretching Sheet, *Boundary Value Problems*, 2013, 136

[28] Brewster and M.Q. 1992 Thermal Radiative Transfer and Properties, *John Wiley & Sons*, NewYork

[29] Khan, W.A., Aziz and A. 2011 Double-diffusive Natural Convective Boundary Layer Flow in a Porous Medium Saturated with a Nanofluid over a Vertical Plate: Prescribed Surface Heat, Solute and Nanoparticle Fluxes, *Int. J. Therm. Sci*. Vol.**50** pp.2154-2160

[30] Na and T.Y. 1979 Computational Methods in Engineering Boundary Value Problems, *Academic Press*, New York